Moderate and extreme urban rainfall modeling at a fine spatio-temporal resolution

Occimaths, Toulouse, December 2024

Chloé SERRE-COMBE [1] Nicolas MEYER [1] Thomas OPITZ [2] Gwladys TOULEMONDE [1]

[1] *IMAG, Université de Montpellier, LEMON Inria*

[2] *INRAE, BioSP, Avignon*

Floods in Montpellier, September 2022 and August 2015 (*Midi Libre*)

- Mediterranean events, localized rainfall
- Urban area, flood risks

Study area

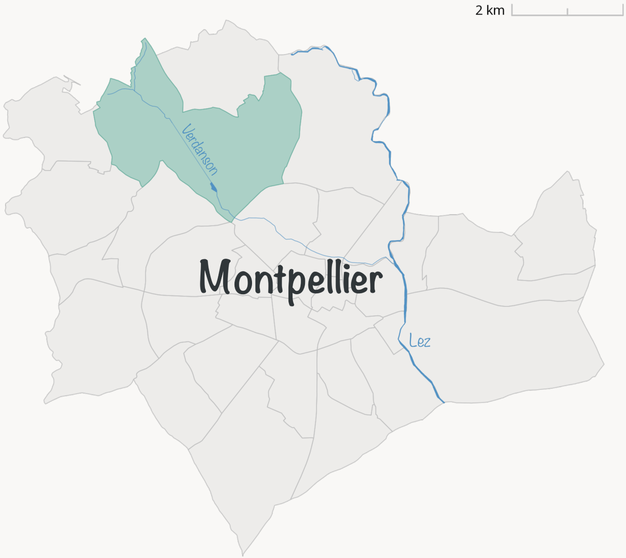

- North of Montpellier, *Hôpitaux-Facultés* district
- Verdanson water catchment, tributary of the Lez river

Rain gauges network

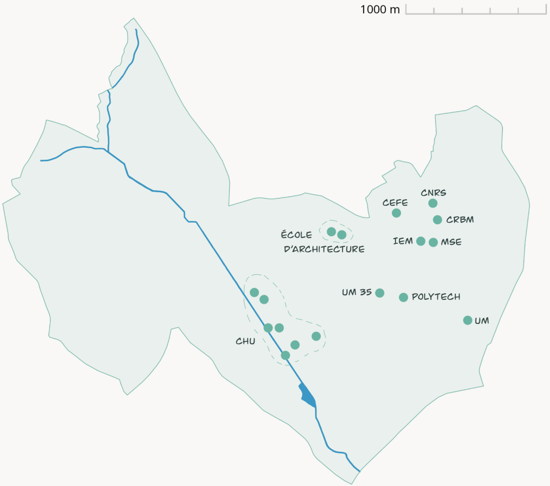

- **Source:** Urban observatory of HydroScience Montpellier (OHSM)[1]
- **Time period:** [2019, 2023]
- **Temp. resol.:** 5 minutes
- **Spatial resol.:** 77 m to 1531 m

[1] Finaud-Guyot et al. 2023

$\mathcal{S} = \{\textbf{17 rain gauges}\} \subset \mathbb{R}^2$ and $\mathcal{T} \subset \mathbb{R}_+$

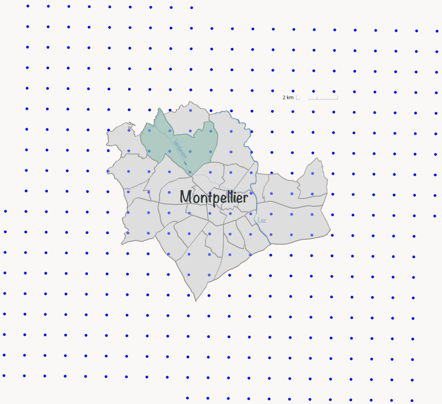

- **Source:** COMEPHORE, Météo France
- **Time period:** [1997, 2023]
- **Temporal resolution:** Every hour
- **Spatial resolution:** 1 km^2

$\mathcal{S} = \{\textbf{400 pixels}\} \subset \mathbb{R}^2$ and $\mathcal{T} \subset \mathbb{R}_+$

More consistent data: HSM + COMEPHORE and Neural Network Downscaling.

Univariate precipitation modeling

Extreme precipitation

Block-maxima

Peaks Over Threshold

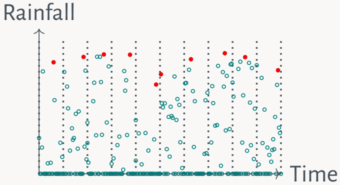

Generalized Extreme Value distribution (GEV)

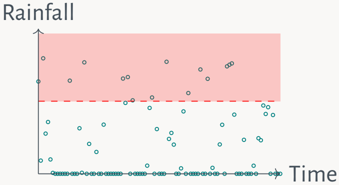

Generalized Pareto Distribution (GPD)

Generalized Pareto Distribution

$$\overline{H}_\xi\left(\frac{x-u}{\sigma}\right) = \begin{cases} \left(1+\xi\frac{x-u}{\sigma}\right)_+^{-1/\xi} & \text{if } \xi \neq 0\,, \\ e^{-\frac{x-u}{\sigma}} & \text{if } \xi = 0\,, \end{cases}$$

where $a_+ = \max(a, 0)$, $\sigma > 0$, $x - u > 0$

- Models extreme precipitation
- Depends on a threshold choice

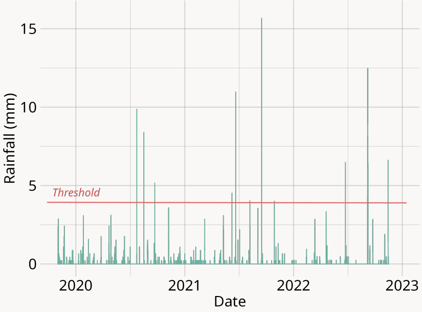

Generalized Pareto Distribution ⟶ **Extended GPD**[2]

$$\overline{H}_\xi\left(\frac{x-u}{\sigma}\right) = \begin{cases} \left(1+\xi\frac{x-u}{\sigma}\right)_+^{-1/\xi} & \text{if } \xi \neq 0\,, \\ e^{-\frac{x-u}{\sigma}} & \text{if } \xi = 0\,, \end{cases}$$

where $a_+ = \max(a, 0)$, $\sigma > 0$, $x - u > 0$

- Models extreme precipitation
- Depends on a threshold choice

$$F(x) = G\left(H_\xi\left(\frac{x}{\sigma}\right)\right),$$

where $G(x) = x^\kappa$, $\kappa > 0$

- Models **moderate and extreme** precipitation
- Avoids a threshold choice

[2] Naveau et al. 2016

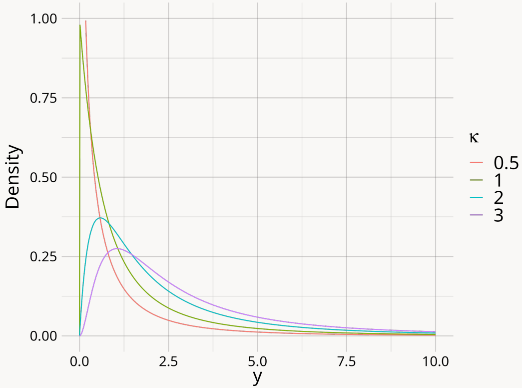

$\sigma = 1,\ \xi = 0.5$

Extended GPD

$$F(x) = G\left(H_\xi\left(\frac{x}{\sigma}\right)\right),$$

where $G(x) = x^\kappa,\ \kappa > 0$

- Models **moderate and extreme** precipitation
- Avoids a threshold choice

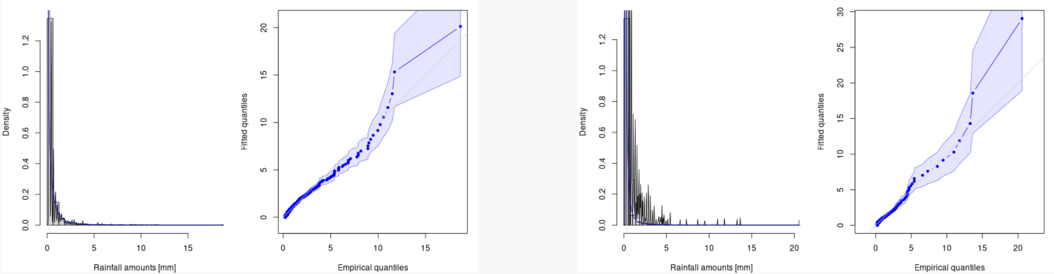

EGPD fitting for two rain gauges, CRBM (left) and CNRS (right) with left-censoring and 95% CI

EGPD FITTING

Left-censoring: selected according to the NRMSE criterion for each site individually[3]

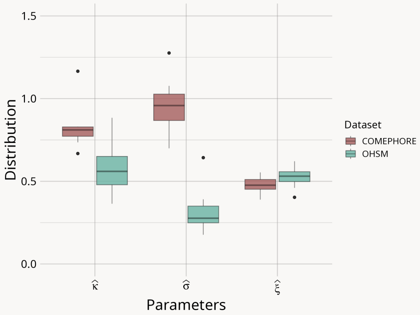

Parameter estimates

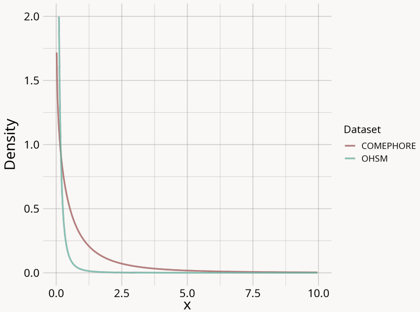

Density with mean parameters

[3] Haruna, Blanchet, and Favre 2023

Rainfall field: $\boldsymbol{X} = \{X_{\boldsymbol{s},t}\,,\ (\boldsymbol{s},t) \in \mathcal{S} \times \mathcal{T}\}$ stationary and isotropic

Max-stable Brown-Resnick process

For all $\boldsymbol{s} \in \mathcal{S}$ and $t \in \mathcal{T}$,

$$X_{\boldsymbol{s},t} = \bigvee_{j=1}^{\infty} \xi_j e^{W^j_{\boldsymbol{s},t} - \gamma(\boldsymbol{s},t)}$$

- ξ_j: point of a Poisson process with intensity $\xi^{-2}d\xi$
- W^j: independent replicates of an intrinsic stationary and isotropic Gaussian random field $\boldsymbol{W}$
- γ: spatio-temporal variogram of $\boldsymbol{W}$

r-Pareto process

For all $\boldsymbol{s} \in \mathcal{S}$ and $t \in \mathcal{T}$, a risk function $r(X) = X_{\boldsymbol{s}_0,t_0}$,

$$X_{\boldsymbol{s},t} \mid X_{\boldsymbol{s}_0,t_0} > u \xrightarrow{d} Z_{\boldsymbol{s},t} \quad \text{with} \quad Z_{\boldsymbol{s},t} = uR_{\boldsymbol{s},t} e^{W_{\boldsymbol{s},t} - W_{\boldsymbol{s}_0,t_0} - \gamma(\boldsymbol{s}-\boldsymbol{s}_0, t-t_0)},$$

with $(\boldsymbol{s}_0, t_0)$ a given space-time location, u a high threshold and $R \sim \mathit{Pareto}(1)$.

Dependence measures

Let $\Lambda_{\mathcal{S}} \subset \mathbb{R}_+^2$ and $\Lambda_{\mathcal{T}} \subset \mathbb{R}_+$ be sets of spatial and temporal lags respectively.

Spatio-temporal extremogram

For all $\boldsymbol{h} \in \Lambda_{\mathcal{S}}, \tau \in \Lambda_{\mathcal{T}}$,

$$\chi(\boldsymbol{h}, \tau) = \lim_{q \to 1} \mathbb{P}(X^*_{\boldsymbol{s},t} > q \mid X^*_{\boldsymbol{s}+\boldsymbol{h},t+\tau} > q),$$

with $q \in [0, 1[$ and $X^*_{\boldsymbol{s},t}$ the uniform margins.

Spatio-temporal variogram γ

$$\gamma(\boldsymbol{h}, \tau) = \frac{1}{2} Var\left(W_{\boldsymbol{s},t} - W_{\boldsymbol{s}+\boldsymbol{h},t+\tau}\right), \ \boldsymbol{h} \in \Lambda_{\mathcal{S}}, \tau \in \Lambda_{\mathcal{T}}$$

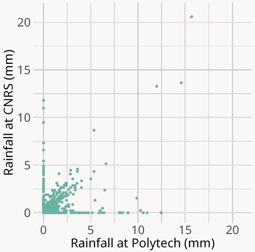

Let $\Lambda_{\mathcal{S}} \subset \mathbb{R}_+^2$ and $\Lambda_{\mathcal{T}} \subset \mathbb{R}_+$ be sets of spatial and temporal lags respectively.

Spatio-temporal extremogram

For all $\boldsymbol{h} \in \Lambda_{\mathcal{S}}, \tau \in \Lambda_{\mathcal{T}}$,

$$\chi(\boldsymbol{h}, \tau) = \lim_{q \to 1} \mathbb{P}(X^*_{\boldsymbol{s},t} > q \mid X^*_{\boldsymbol{s}+\boldsymbol{h},t+\tau} > q),$$

with $q \in [0, 1[$ and $X^*_{\boldsymbol{s},t}$ the uniform margins.

Spatio-temporal variogram γ

$$\gamma(\boldsymbol{h}, \tau) = \frac{1}{2} Var\left(W_{\boldsymbol{s},t} - W_{\boldsymbol{s}+\boldsymbol{h},t+\tau}\right), \ \boldsymbol{h} \in \Lambda_{\mathcal{S}}, \tau \in \Lambda_{\mathcal{T}}$$

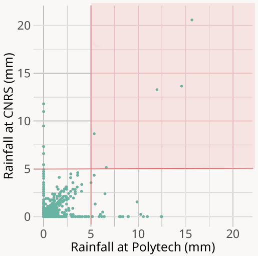

Spatio-temporal extremogram with a Brown-Resnick dependence

Let $\boldsymbol{h} \in \Lambda_{\mathcal{S}}$ and $\tau \in \Lambda_{\mathcal{T}}$. We have

$$\chi(\boldsymbol{h}, \tau) = 2\left(1 - \phi\left(\sqrt{\frac{1}{2}\gamma(\boldsymbol{h}, \tau)}\right)\right)$$

with ϕ the std normal c.d.f. and γ the variogram of $\boldsymbol{W}$.

First dependence framework: Buhl et al. 2019

Case of additive separability: $\frac{\gamma(\boldsymbol{h},\tau)}{2} = \beta_1 ||\boldsymbol{h}||^{\alpha_1} + \beta_2 |\tau|^{\alpha_2}$, $0 < \alpha_1, \alpha_2 \leq 2\,,\ \beta_1, \beta_2 > 0$

Spatio-temporal

$$\chi(\boldsymbol{h},\tau) = 2\left(1 - \phi\left(\sqrt{\tfrac{1}{2}\gamma(\boldsymbol{h},\tau)}\right)\right)$$

Transformation:

$$\eta(\chi) = 2\log\left(\phi^{-1}\left(1 - \tfrac{1}{2}\chi\right)\right)$$

Spatial

$$\eta\left(\chi(\boldsymbol{h},0)\right) = \log\beta_1 + \alpha_1 \log||\boldsymbol{h}||\,,\ \ \boldsymbol{h} \in \Lambda_{\mathcal{S}}$$

Temporal

$$\eta\left(\chi(0,\tau)\right) = \log\beta_2 + \alpha_2 \log\tau\,,\ \ \tau \in \Lambda_{\mathcal{T}}$$

Case of additive separability: $\frac{\gamma(\boldsymbol{h},\tau)}{2} = \beta_1 ||\boldsymbol{h}||^{\alpha_1} + \beta_2 |\tau|^{\alpha_2}, \; 0 < \alpha_1, \alpha_2 \leq 2\,, \; \beta_1, \beta_2 > 0$

Spatio-temporal

$$\chi(\boldsymbol{h},\tau) = 2\left(1-\phi\left(\sqrt{\tfrac{1}{2}\gamma(\boldsymbol{h},\tau)}\right)\right)$$

Transformation:

$$\eta(\chi) = 2\log\left(\phi^{-1}\left(1-\tfrac{1}{2}\chi\right)\right)$$

Spatial

$$\eta\left(\chi(\boldsymbol{h},0)\right) := c_1 + \alpha_1 x_h\,, \; \boldsymbol{h} \in \Lambda_{\mathcal{S}}$$

Temporal

$$\eta\left(\chi(0,\tau)\right) := c_2 + \alpha_2 x_\tau\,, \; \tau \in \Lambda_{\mathcal{T}}$$

Weighted Least Squares Estimation (WLSE)

$$\begin{pmatrix} \widehat{c}_i \\ \widehat{\alpha}_i \end{pmatrix} = \operatorname{argmin}_{c_i,\alpha_i} \sum_x w_x \left(\eta\left(\widehat{\chi}\right) - (c_i + \alpha_i x)\right)^2$$

Brown-Resnick simulations

- Spatial: $\mathcal{S} = \{\text{400 sites}\}$, $\mathcal{T} = \{1, \ldots, 50\}$, $|\Lambda_{\mathcal{S}}| = 10$ and $|\Lambda_{\mathcal{T}}| = 10$
- Temporal: $\mathcal{S} = \{\text{25 sites}\}$, $\mathcal{T} = \{1, \ldots, 300\}$, $|\Lambda_{\mathcal{S}}| = 10$ and $|\Lambda_{\mathcal{T}}| = 10$

	True	Mean	RMSE	MAE
$\widehat{\beta}_1$	0.4	0.524	0.138	0.126
$\widehat{\alpha}_1$	1.5	1.507	0.120	0.088
$\widehat{\beta}_2$	0.2	0.259	0.093	0.074
$\widehat{\alpha}_2$	1	0.873	0.149	0.128

Parameter estimates for 100 realisations

True variogram: $\frac{1}{2}\gamma(\boldsymbol{h}, \tau) = 0.4\|\boldsymbol{h}\|^{3/2} + 0.2|\tau|$

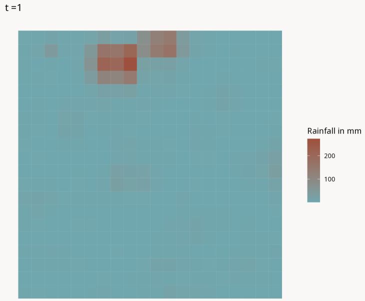

Brown-Resnick simulations

- Spatial: $\mathcal{S} = \{\,400 \text{ sites}\,\}$, $\mathcal{T} = \{1, \ldots, 50\}$, $|\Lambda_{\mathcal{S}}| = 10$ and $|\Lambda_{\mathcal{T}}| = 10$
- Temporal: $\mathcal{S} = \{\,25 \text{ sites}\,\}$, $\mathcal{T} = \{1, \ldots, 300\}$, $|\Lambda_{\mathcal{S}}| = 10$ and $|\Lambda_{\mathcal{T}}| = 10$

	True	Mean	RMSE	MAE
$\widehat{\beta}_1$	0.4	0.524	0.138	0.126
$\widehat{\alpha}_1$	1.5	1.507	0.120	0.088
$\widehat{\beta}_2$	0.2	0.259	0.093	0.074
$\widehat{\alpha}_2$	1	0.873	0.149	0.128

Parameter estimates for 100 realisations

True variogram: $\frac{1}{2}\gamma\left(\boldsymbol{h}, \tau\right) = 0.4\|\boldsymbol{h}\|^{3/2} + 0.2|\tau|$

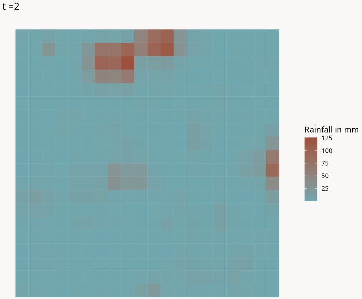

Brown-Resnick simulations

- Spatial: $\mathcal{S} = \{\,400 \text{ sites}\,\}$, $\mathcal{T} = \{1, \ldots, 50\}$, $|\Lambda_{\mathcal{S}}| = 10$ and $|\Lambda_{\mathcal{T}}| = 10$
- Temporal: $\mathcal{S} = \{\,25 \text{ sites}\,\}$, $\mathcal{T} = \{1, \ldots, 300\}$, $|\Lambda_{\mathcal{S}}| = 10$ and $|\Lambda_{\mathcal{T}}| = 10$

	True	Mean	RMSE	MAE
$\widehat{\beta}_1$	0.4	0.524	0.138	0.126
$\widehat{\alpha}_1$	1.5	1.507	0.120	0.088
$\widehat{\beta}_2$	0.2	0.259	0.093	0.074
$\widehat{\alpha}_2$	1	0.873	0.149	0.128

Parameter estimates for 100 realisations

True variogram: $\frac{1}{2}\gamma\left(\boldsymbol{h}, \tau\right) = 0.4\|\boldsymbol{h}\|^{3/2} + 0.2|\tau|$

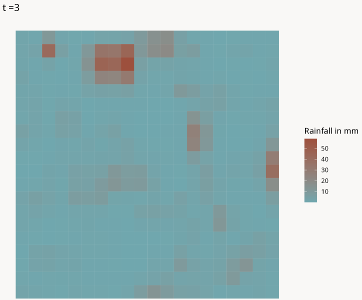

Model validation - simulations

Brown-Resnick simulations

- Spatial: $\mathcal{S} = \{\text{400 sites}\}$, $\mathcal{T} = \{1, \ldots, 50\}$, $|\Lambda_{\mathcal{S}}| = 10$ and $|\Lambda_{\mathcal{T}}| = 10$
- Temporal: $\mathcal{S} = \{\text{25 sites}\}$, $\mathcal{T} = \{1, \ldots, 300\}$, $|\Lambda_{\mathcal{S}}| = 10$ and $|\Lambda_{\mathcal{T}}| = 10$

	True	Mean	RMSE	MAE
$\widehat{\beta}_1$	0.4	0.524	0.138	0.126
$\widehat{\alpha}_1$	1.5	1.507	0.120	0.088
$\widehat{\beta}_2$	0.2	0.259	0.093	0.074
$\widehat{\alpha}_2$	1	0.873	0.149	0.128

Parameter estimates for 100 realisations

True variogram: $\frac{1}{2}\gamma(\boldsymbol{h}, \tau) = 0.4\|\boldsymbol{h}\|^{3/2} + 0.2|\tau|$

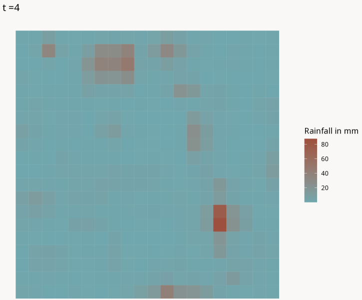

Brown-Resnick simulations

- Spatial: $\mathcal{S} = \{\,400 \text{ sites}\,\}$, $\mathcal{T} = \{1, \ldots, 50\}$, $|\Lambda_{\mathcal{S}}| = 10$ and $|\Lambda_{\mathcal{T}}| = 10$
- Temporal: $\mathcal{S} = \{\,25 \text{ sites}\,\}$, $\mathcal{T} = \{1, \ldots, 300\}$, $|\Lambda_{\mathcal{S}}| = 10$ and $|\Lambda_{\mathcal{T}}| = 10$

	True	Mean	RMSE	MAE
$\widehat{\beta}_1$	0.4	0.524	0.138	0.126
$\widehat{\alpha}_1$	1.5	1.507	0.120	0.088
$\widehat{\beta}_2$	0.2	0.259	0.093	0.074
$\widehat{\alpha}_2$	1	0.873	0.149	0.128

Parameter estimates for 100 realisations

True variogram: $\frac{1}{2}\gamma\left(\boldsymbol{h}, \tau\right) = 0.4\|\boldsymbol{h}\|^{3/2} + 0.2|\tau|$

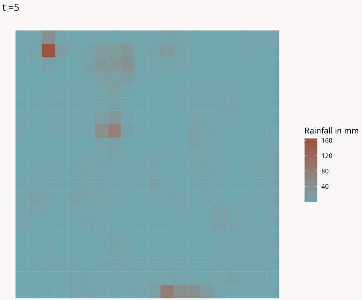

Brown-Resnick simulations

- Spatial: $\mathcal{S} = \{\,400 \text{ sites}\,\}$, $\mathcal{T} = \{1, \dots, 50\}$, $|\Lambda_{\mathcal{S}}| = 10$ and $|\Lambda_{\mathcal{T}}| = 10$
- Temporal: $\mathcal{S} = \{\,25 \text{ sites}\,\}$, $\mathcal{T} = \{1, \dots, 300\}$, $|\Lambda_{\mathcal{S}}| = 10$ and $|\Lambda_{\mathcal{T}}| = 10$

	True	Mean	RMSE	MAE
$\widehat{\beta}_1$	0.4	0.524	0.138	0.126
$\widehat{\alpha}_1$	1.5	1.507	0.120	0.088
$\widehat{\beta}_2$	0.2	0.259	0.093	0.074
$\widehat{\alpha}_2$	1	0.873	0.149	0.128

Parameter estimates for 100 realisations

True variogram: $\frac{1}{2}\gamma\left(\boldsymbol{h}, \tau\right) = 0.4\|\boldsymbol{h}\|^{3/2} + 0.2|\tau|$

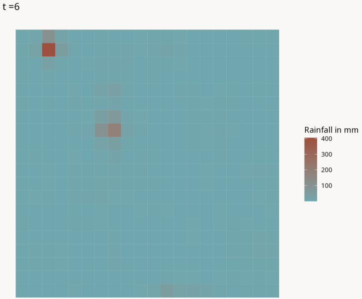

Model validation - simulations

Brown-Resnick simulations

- Spatial: $\mathcal{S} = \{\text{ 400 sites }\}$, $\mathcal{T} = \{1, \dots, 50\}$, $|\Lambda_{\mathcal{S}}| = 10$ and $|\Lambda_{\mathcal{T}}| = 10$
- Temporal: $\mathcal{S} = \{\text{ 25 sites }\}$, $\mathcal{T} = \{1, \dots, 300\}$, $|\Lambda_{\mathcal{S}}| = 10$ and $|\Lambda_{\mathcal{T}}| = 10$

	True	Mean	RMSE	MAE
$\widehat{\beta}_1$	0.4	0.524	0.138	0.126
$\widehat{\alpha}_1$	1.5	1.507	0.120	0.088
$\widehat{\beta}_2$	0.2	0.259	0.093	0.074
$\widehat{\alpha}_2$	1	0.873	0.149	0.128

Parameter estimates for 100 realisations

True variogram: $\frac{1}{2}\gamma(\boldsymbol{h}, \tau) = 0.4\|\boldsymbol{h}\|^{3/2} + 0.2|\tau|$

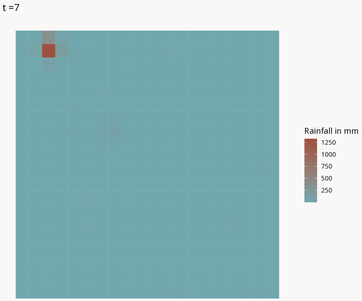

Brown-Resnick simulations

- Spatial: $\mathcal{S} = \{\,400 \text{ sites}\,\}$, $\mathcal{T} = \{1, \ldots, 50\}$, $|\Lambda_{\mathcal{S}}| = 10$ and $|\Lambda_{\mathcal{T}}| = 10$
- Temporal: $\mathcal{S} = \{\,25 \text{ sites}\,\}$, $\mathcal{T} = \{1, \ldots, 300\}$, $|\Lambda_{\mathcal{S}}| = 10$ and $|\Lambda_{\mathcal{T}}| = 10$

	True	Mean	RMSE	MAE
$\widehat{\beta}_1$	0.4	0.524	0.138	0.126
$\widehat{\alpha}_1$	1.5	1.507	0.120	0.088
$\widehat{\beta}_2$	0.2	0.259	0.093	0.074
$\widehat{\alpha}_2$	1	0.873	0.149	0.128

Parameter estimates for 100 realisations

True variogram: $\frac{1}{2}\gamma\left(\boldsymbol{h}, \tau\right) = 0.4\|\boldsymbol{h}\|^{3/2} + 0.2|\tau|$

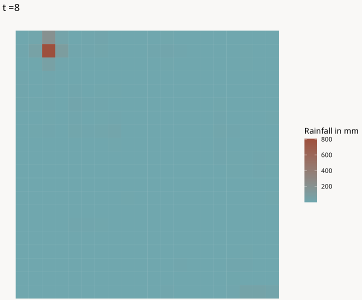

Brown-Resnick simulations

- Spatial: $\mathcal{S} = \{\text{ 400 sites }\}$, $\mathcal{T} = \{1, \ldots, 50\}$, $|\Lambda_{\mathcal{S}}| = 10$ and $|\Lambda_{\mathcal{T}}| = 10$
- Temporal: $\mathcal{S} = \{\text{ 25 sites }\}$, $\mathcal{T} = \{1, \ldots, 300\}$, $|\Lambda_{\mathcal{S}}| = 10$ and $|\Lambda_{\mathcal{T}}| = 10$

	True	Mean	RMSE	MAE
$\widehat{\beta}_1$	0.4	0.524	0.138	0.126
$\widehat{\alpha}_1$	1.5	1.507	0.120	0.088
$\widehat{\beta}_2$	0.2	0.259	0.093	0.074
$\widehat{\alpha}_2$	1	0.873	0.149	0.128

Parameter estimates for 100 realisations

True variogram: $\frac{1}{2}\gamma\left(\boldsymbol{h}, \tau\right) = 0.4\|\boldsymbol{h}\|^{3/2} + 0.2|\tau|$

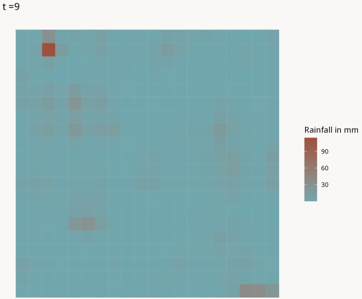

Model validation - simulations

Brown-Resnick simulations

- Spatial: $\mathcal{S} = \{\text{400 sites}\}$, $\mathcal{T} = \{1, \ldots, 50\}$, $|\Lambda_{\mathcal{S}}| = 10$ and $|\Lambda_{\mathcal{T}}| = 10$
- Temporal: $\mathcal{S} = \{\text{25 sites}\}$, $\mathcal{T} = \{1, \ldots, 300\}$, $|\Lambda_{\mathcal{S}}| = 10$ and $|\Lambda_{\mathcal{T}}| = 10$

	True	Mean	RMSE	MAE
$\widehat{\beta}_1$	0.4	0.524	0.138	0.126
$\widehat{\alpha}_1$	1.5	1.507	0.120	0.088
$\widehat{\beta}_2$	0.2	0.259	0.093	0.074
$\widehat{\alpha}_2$	1	0.873	0.149	0.128

Parameter estimates for 100 realisations

True variogram: $\frac{1}{2}\gamma(\boldsymbol{h}, \tau) = 0.4\|\boldsymbol{h}\|^{3/2} + 0.2|\tau|$

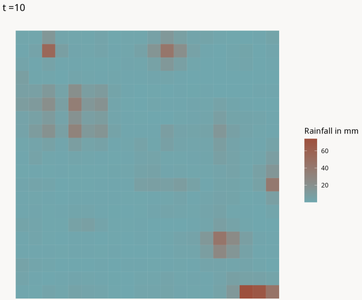

Model validation - simulations

Brown-Resnick simulations

- Spatial: $\mathcal{S} = \{\text{ 400 sites }\}$, $\mathcal{T} = \{1, \ldots, 50\}$, $|\Lambda_{\mathcal{S}}| = 10$ and $|\Lambda_{\mathcal{T}}| = 10$
- Temporal: $\mathcal{S} = \{\text{ 25 sites }\}$, $\mathcal{T} = \{1, \ldots, 300\}$, $|\Lambda_{\mathcal{S}}| = 10$ and $|\Lambda_{\mathcal{T}}| = 10$

	True	Mean	RMSE	MAE
$\widehat{\beta}_1$	0.4	0.524	0.138	0.126
$\widehat{\alpha}_1$	1.5	1.507	0.120	0.088
$\widehat{\beta}_2$	0.2	0.259	0.093	0.074
$\widehat{\alpha}_2$	1	0.873	0.149	0.128

Parameter estimates for 100 realisations

True variogram: $\frac{1}{2}\gamma\left(\boldsymbol{h}, \tau\right) = 0.4\|\boldsymbol{h}\|^{3/2} + 0.2|\tau|$

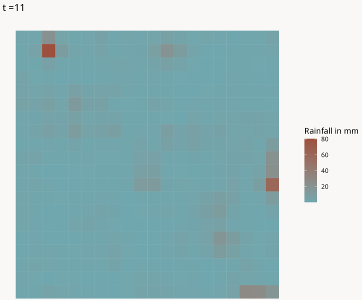

Model validation - simulations

Brown-Resnick simulations

- Spatial: $\mathcal{S} = \{\,400 \text{ sites}\,\}$, $\mathcal{T} = \{1, \dots, 50\}$, $|\Lambda_{\mathcal{S}}| = 10$ and $|\Lambda_{\mathcal{T}}| = 10$
- Temporal: $\mathcal{S} = \{\,25 \text{ sites}\,\}$, $\mathcal{T} = \{1, \dots, 300\}$, $|\Lambda_{\mathcal{S}}| = 10$ and $|\Lambda_{\mathcal{T}}| = 10$

	True	Mean	RMSE	MAE
$\widehat{\beta}_1$	0.4	0.524	0.138	0.126
$\widehat{\alpha}_1$	1.5	1.507	0.120	0.088
$\widehat{\beta}_2$	0.2	0.259	0.093	0.074
$\widehat{\alpha}_2$	1	0.873	0.149	0.128

Parameter estimates for 100 realisations

True variogram: $\frac{1}{2}\gamma(\boldsymbol{h}, \tau) = 0.4\|\boldsymbol{h}\|^{3/2} + 0.2|\tau|$

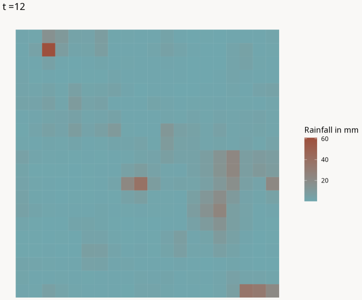

Brown-Resnick simulations

- Spatial: $\mathcal{S} = \{\,400 \text{ sites}\,\}$, $\mathcal{T} = \{1, \ldots, 50\}$, $|\Lambda_{\mathcal{S}}| = 10$ and $|\Lambda_{\mathcal{T}}| = 10$
- Temporal: $\mathcal{S} = \{\,25 \text{ sites}\,\}$, $\mathcal{T} = \{1, \ldots, 300\}$, $|\Lambda_{\mathcal{S}}| = 10$ and $|\Lambda_{\mathcal{T}}| = 10$

	True	Mean	RMSE	MAE
$\widehat{\beta}_1$	0.4	0.524	0.138	0.126
$\widehat{\alpha}_1$	1.5	1.507	0.120	0.088
$\widehat{\beta}_2$	0.2	0.259	0.093	0.074
$\widehat{\alpha}_2$	1	0.873	0.149	0.128

Parameter estimates for 100 realisations

True variogram: $\frac{1}{2}\gamma\left(\boldsymbol{h}, \tau\right) = 0.4\|\boldsymbol{h}\|^{3/2} + 0.2|\tau|$

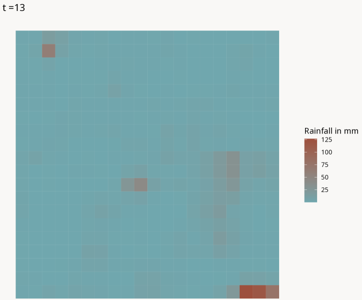

Model validation - simulations

Brown-Resnick simulations

- Spatial: $\mathcal{S} = \{\,400 \text{ sites}\,\}$, $\mathcal{T} = \{1, \ldots, 50\}$, $|\Lambda_{\mathcal{S}}| = 10$ and $|\Lambda_{\mathcal{T}}| = 10$
- Temporal: $\mathcal{S} = \{\,25 \text{ sites}\,\}$, $\mathcal{T} = \{1, \ldots, 300\}$, $|\Lambda_{\mathcal{S}}| = 10$ and $|\Lambda_{\mathcal{T}}| = 10$

	True	Mean	RMSE	MAE
$\widehat{\beta}_1$	0.4	0.524	0.138	0.126
$\widehat{\alpha}_1$	1.5	1.507	0.120	0.088
$\widehat{\beta}_2$	0.2	0.259	0.093	0.074
$\widehat{\alpha}_2$	1	0.873	0.149	0.128

Parameter estimates for 100 realisations

True variogram: $\frac{1}{2}\gamma\left(\boldsymbol{h}, \tau\right) = 0.4\|\boldsymbol{h}\|^{3/2} + 0.2|\tau|$

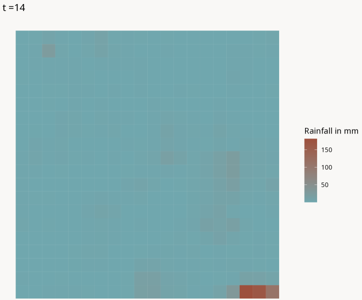

Brown-Resnick simulations

- Spatial: $\mathcal{S} = \{\,400 \text{ sites}\,\}$, $\mathcal{T} = \{1, \dots, 50\}$, $|\Lambda_{\mathcal{S}}| = 10$ and $|\Lambda_{\mathcal{T}}| = 10$
- Temporal: $\mathcal{S} = \{\,25 \text{ sites}\,\}$, $\mathcal{T} = \{1, \dots, 300\}$, $|\Lambda_{\mathcal{S}}| = 10$ and $|\Lambda_{\mathcal{T}}| = 10$

	True	Mean	RMSE	MAE
$\widehat{\beta}_1$	0.4	0.524	0.138	0.126
$\widehat{\alpha}_1$	1.5	1.507	0.120	0.088
$\widehat{\beta}_2$	0.2	0.259	0.093	0.074
$\widehat{\alpha}_2$	1	0.873	0.149	0.128

Parameter estimates for 100 realisations

True variogram: $\frac{1}{2}\gamma\left(\boldsymbol{h}, \tau\right) = 0.4\|\boldsymbol{h}\|^{3/2} + 0.2|\tau|$

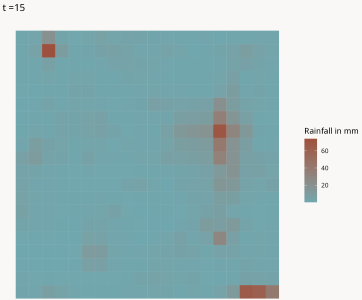

Model validation - simulations

Brown-Resnick simulations

- Spatial: $\mathcal{S} = \{\text{ 400 sites }\}$, $\mathcal{T} = \{1, \ldots, 50\}$, $|\Lambda_\mathcal{S}| = 10$ and $|\Lambda_\mathcal{T}| = 10$
- Temporal: $\mathcal{S} = \{\text{ 25 sites }\}$, $\mathcal{T} = \{1, \ldots, 300\}$, $|\Lambda_\mathcal{S}| = 10$ and $|\Lambda_\mathcal{T}| = 10$

	True	Mean	RMSE	MAE
$\widehat{\beta}_1$	0.4	0.524	0.138	0.126
$\widehat{\alpha}_1$	1.5	1.507	0.120	0.088
$\widehat{\beta}_2$	0.2	0.259	0.093	0.074
$\widehat{\alpha}_2$	1	0.873	0.149	0.128

Parameter estimates for 100 realisations

True variogram: $\frac{1}{2}\gamma(\boldsymbol{h}, \tau) = 0.4\|\boldsymbol{h}\|^{3/2} + 0.2|\tau|$

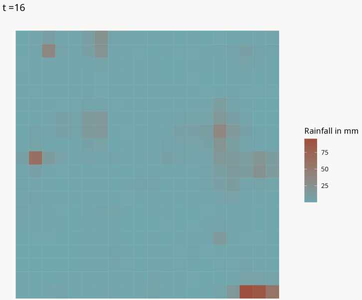

Spatial dependence estimation

Empirical spatial extremogram

For a fixed $t \in \mathcal{T}$ and q a high quantile,

$$\widehat{\chi}_q^{(t)}(\boldsymbol{h}, 0) = \frac{\frac{1}{|N_{\boldsymbol{h}}|} \sum_{i,j \,|\, (\boldsymbol{s}_i, \boldsymbol{s}_j) \in N_{\boldsymbol{h}}} \mathbb{1}_{\{X^*_{\boldsymbol{s}_i,t} > q \,, X^*_{\boldsymbol{s}_j,t} > q\}}}{\frac{1}{|\mathcal{S}|} \sum_{i=1}^{|\mathcal{S}|} \mathbb{1}_{\{X^*_{\boldsymbol{s}_i,t} > q\}}},$$

where $C_{\boldsymbol{h}}$ are equifrequent distance classes and $N_{\boldsymbol{h}} = \left\{ (\boldsymbol{s}_i, \boldsymbol{s}_j) \in \mathcal{S}^2 \;\middle|\; \|\boldsymbol{s}_i - \boldsymbol{s}_j\| \in C_{\boldsymbol{h}} \right\}.$

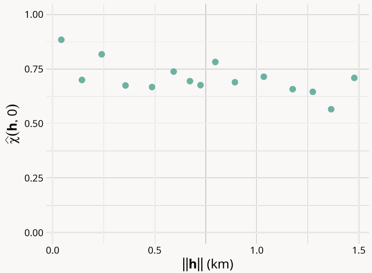

Transformation and WLSE

$\Longrightarrow$

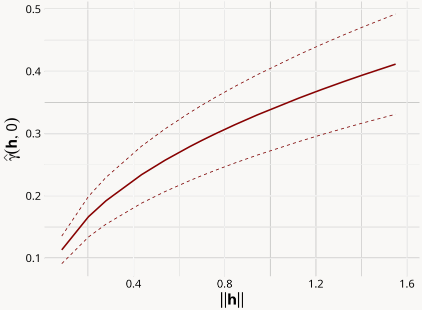

Spatial variogram $\widehat{\gamma}(\boldsymbol{h}, 0) = 2\widehat{\beta}_1 \|\boldsymbol{h}\|^{\widehat{\alpha}_1}$

Temporal dependence estimation

Empirical temporal extremogram

For a location $s \in \mathcal{S}$, a high quantile q and $t_k \in \{t_1, \ldots, t_T\}$,

$$\widehat{\chi}_q^{(s)}(0,\tau) = \frac{\frac{1}{T-\tau}\sum_{k=1}^{T-\tau} \mathbb{1}_{\{X^*_{s,t_k}>q\,,X^*_{s,t_k+\tau}>q\}}}{\frac{1}{T}\sum_{k=1}^{T} \mathbb{1}_{\{X^*_{s,t_k}>q\}}}$$

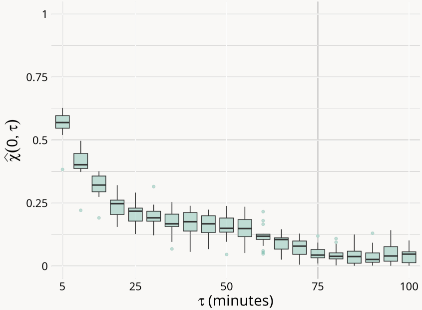

Transformation and WLSE

$\Longrightarrow$

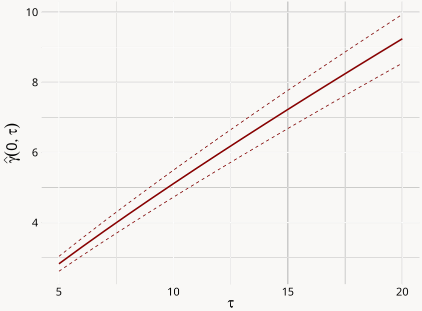

Temporal variogram $\widehat{\gamma}(0,\tau) = 2\widehat{\beta}_2|\tau|^{\widehat{\alpha}_2}$

Advection vector $\boldsymbol{V}$

- Horizontal transport of air masses
- To relax the separability assumption

Lagrangian/Eulerian variogram

$$\gamma_L(\boldsymbol{h}, \tau) = \gamma(\boldsymbol{h} - \tau \boldsymbol{V}, \tau)$$

Dependence model

$$\frac{1}{2}\gamma_L(\boldsymbol{h}, \tau) = \beta_1 \|\boldsymbol{h} - \tau \boldsymbol{V}\|^{\alpha_1} + \beta_2 |\tau|^{\alpha_2}$$

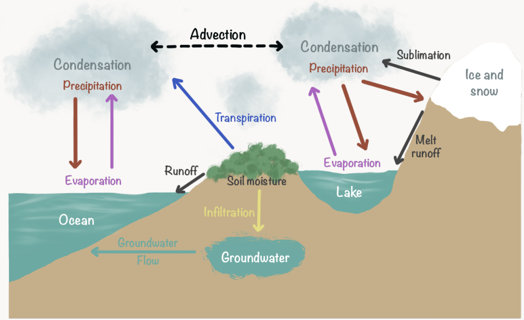

Hydrologic cycle

Advection vector $\boldsymbol{V}$

- Horizontal transport of air masses
- To relax the separability assumption

Lagrangian/Eulerian variogram

$$\gamma_L(\boldsymbol{h}, \tau) = \gamma(\boldsymbol{h} - \tau \boldsymbol{V}, \tau)$$

Dependence model

$$\frac{1}{2}\gamma_L(\boldsymbol{h}, \tau) = \beta_1 \|\boldsymbol{h} - \tau \boldsymbol{V}\|^{\alpha_1} + \beta_2 |\tau|^{\alpha_2}$$

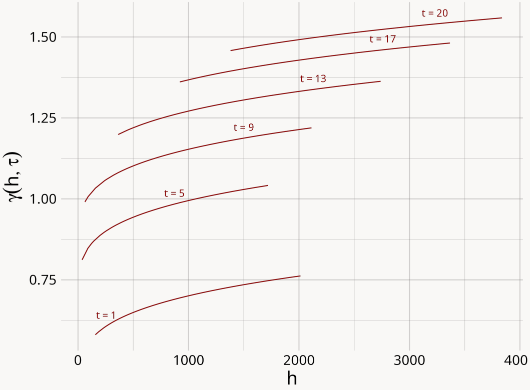

Spatial variogram with a constant advection $\boldsymbol{V} = (0.001, 45)^T$ on OHSM data

Parameter optimization of $\boldsymbol{\Theta} = (\beta_1, \beta_2, \alpha_1, \alpha_2, \boldsymbol{V})$

Joint excesses:

$$\begin{aligned} k_{\boldsymbol{h},\tau} &= \sum_{(\boldsymbol{s}_i,\boldsymbol{s}_j)\in N(\boldsymbol{h})} \sum_{(t_i,t_j)\in N(\tau)} \mathbb{1}_{\{X^*_{\boldsymbol{s}_i,t_i}>q, X^*_{\boldsymbol{s}_j,t_j}>q\}} \\ &\sim \mathcal{B}\left(|N(\boldsymbol{h})| \times |N(\tau)|, \mathbb{P}(X^*_{\boldsymbol{s},t} > q, X^*_{\boldsymbol{s}+\boldsymbol{h},t+\tau} > q)\right) \end{aligned}$$

Composite log-likelihood for r-Pareto processes:

$$l_C(\boldsymbol{\Theta}) \propto \sum_{\boldsymbol{s}:(\boldsymbol{s},\boldsymbol{s}_0)\in N(\boldsymbol{h})} \sum_{\tau\in\Lambda_{\mathcal{T}}:t-t_0=\tau} k_{\boldsymbol{s},\tau} \log \chi_{r,\boldsymbol{\Theta}}(\boldsymbol{h},\tau) + (1-k_{\boldsymbol{s},\tau}) \log(1-\chi_{r,\boldsymbol{\Theta}}(\boldsymbol{h},\tau))$$

where $\chi_{r,\boldsymbol{\Theta}}(\boldsymbol{h},\tau) = \mathbb{P}(X_{\boldsymbol{s}_0+\boldsymbol{h},t_0+\tau} > u)$ is the r-extremogram.

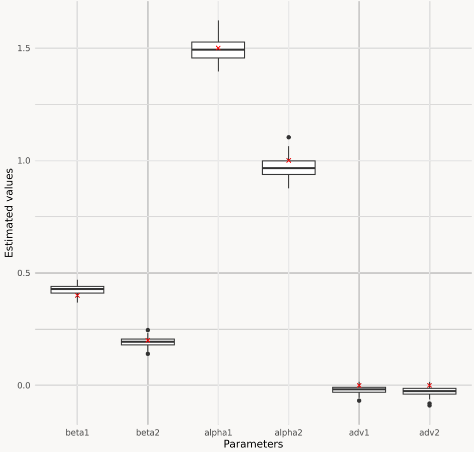

Without advection

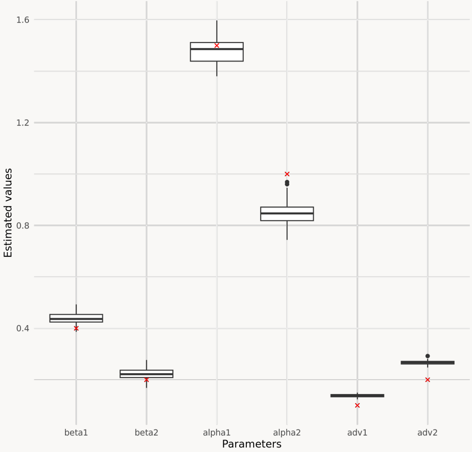

With advection

Parameter estimation on 100 simulations of 100 replicates of r-Pareto processes with 25 sites and 30 time observations

Conclusion

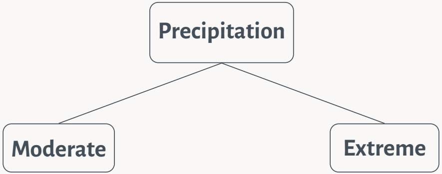

Conclusion

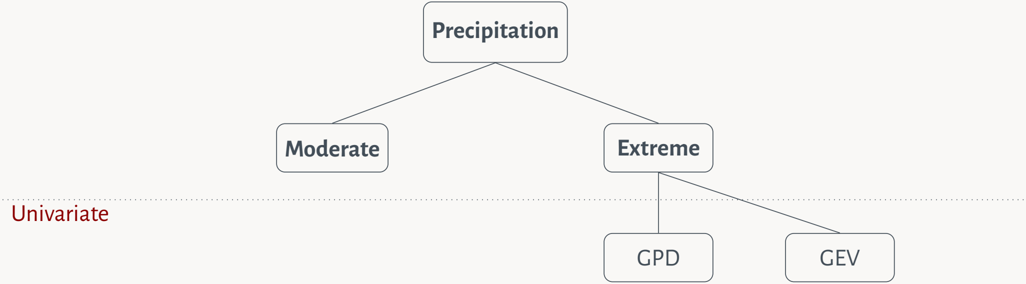

Conclusion

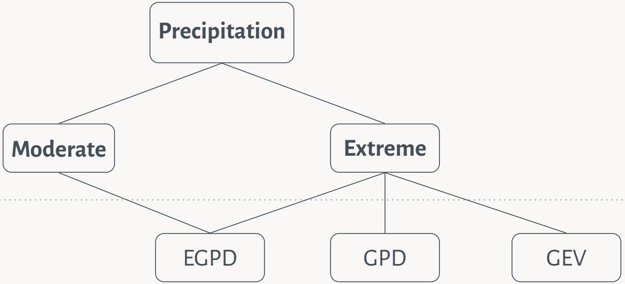

Univariate

Dependence

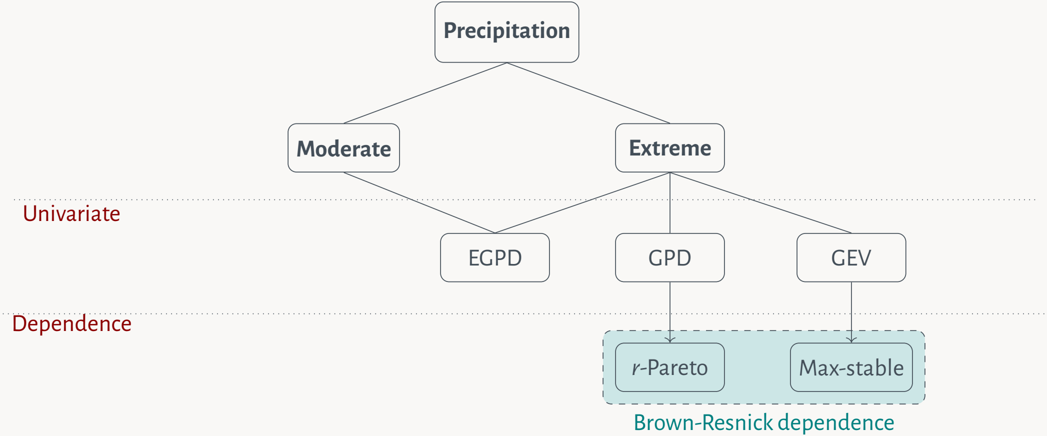
Precipitation
Moderate
Extreme
Univariate
EGPD
GPD
GEV
Dependence
r-Pareto
Max-stable
Brown-Resnick dependence

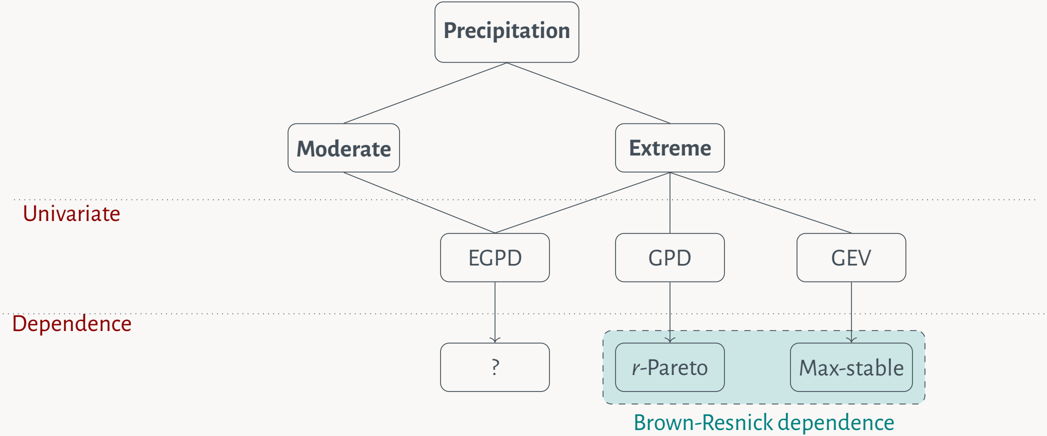
Precipitation
Moderate
Extreme
Univariate
EGPD
GPD
GEV
Dependence
?
r-Pareto
Max-stable
Brown-Resnick dependence

Conclusion

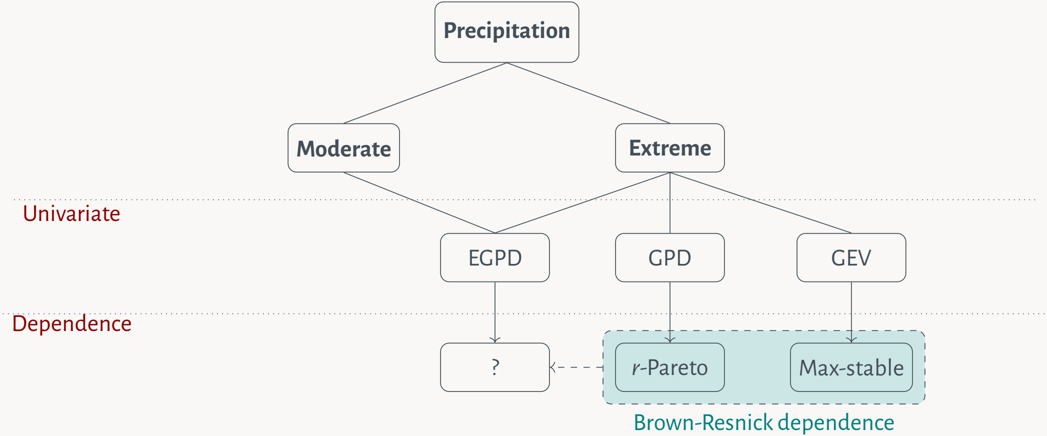

Precipitation
Moderate
Extreme
Univariate
EGPD
GPD
GEV
Dependence
?
r-Pareto
Max-stable
Brown-Resnick dependence

Conclusion

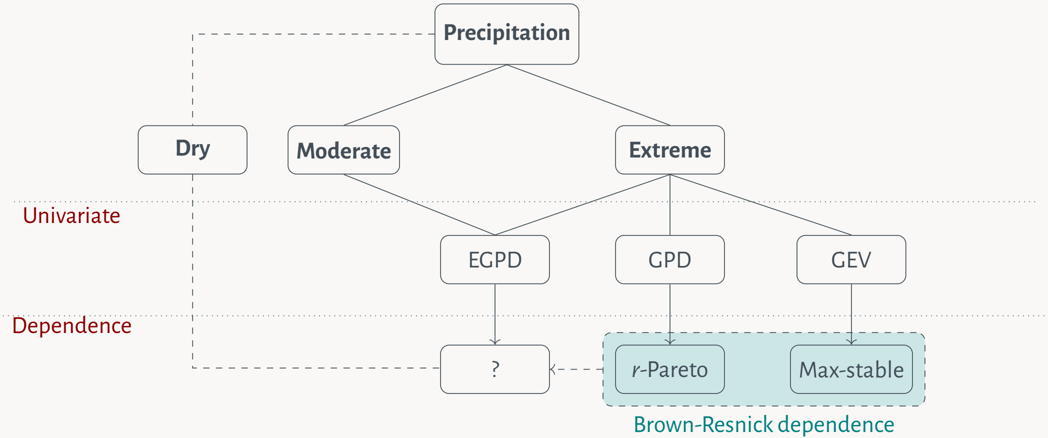

Precipitation
Dry
Moderate
Extreme
Univariate
EGPD
GPD
GEV
Dependence
?
r-Pareto
Max-stable
Brown-Resnick dependence

References

Buhl, Sven et al. (2019). "Semiparametric estimation for isotropic max-stable space-time processes". In: *Bernoulli*.

Finaud-Guyot, Pascal et al. (2023). *Rainfall data collected by the HSM urban observatory (OMSEV)*. doi: 10.23708/67LC36.

Haruna, Abubakar, Juliette Blanchet, and Anne-Catherine Favre (2023). *Modeling Areal Precipitation Hazard: A Data-driven Approach to Model Intensity-Duration-Area-Frequency Relationships using the Full Range of Non-Zero Precipitation in Switzerland*. preprint. Preprints. doi: 10.22541/essoar.169111775.53035997/v1.

Naveau, Philippe et al. (2016). "Modeling jointly low, moderate, and heavy rainfall intensities without a threshold selection". In: *Water Resources Research*. doi: 10.1002/2015WR018552.

Rainfall data - OHSM

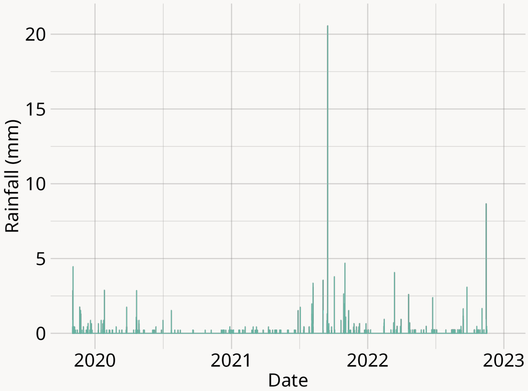

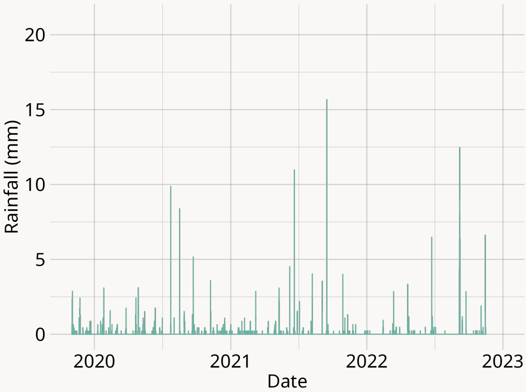

Rainfall amounts on CNRS and Polytech rain gauges